Wave-Optical Reconstruction of Plenoptic Camera Images

André Junker, Tim Stenau, and Karl-Heinz Brenner

Chair for Optoelectronics, University of Heidelberg,
B6 23-29 Bauteil C, 68131 Mannheim, Germany
junker@stud.uni-heidelberg.de

1 Introduction

During the last couple of years light field imaging has become an intensively studied field of research. Unlike a conventional camera, which simply records a two-dimensional spatial intensity distribution, a plenoptic camera additionally measures directional information by incorporating a micro lens array in the optical setup. This allows the image manipulation after the capture to a much greater extent than with conventional images. Typical examples include the refocusing operation, the extension of the depth of field, the calculation of depth information and the reconstruction of parts of the initial object geometry.

These operations all have in common that their software implementation is computationally intensive and requires a large amount of memory. Even up to the late 1990s the hardware available was insufficient to handle the large amount of data, which needed to be processed. Finally it was not before 2005 that a plenoptic camera was built and its images were analyzed and manipulated by computational means based on the ray tracing technique [1].

However, the reconstruction scheme used in [1] suffers from two inherent problems. First, the reconstruction algorithm results in a final image resolution, which is restricted to the number of micro lenses in the micro lens array. Since this number is generally small (typically a factor 10^2 to 10^3 smaller than the sensor resolution), light field images have a rather reduced resolution. Several newer publications [2,3,4] tackle this problem by using a slightly modified camera setup and enhanced image processing techniques. These approaches can be found under the keyword 'super-resolution'. It can be expected, however, that these improvements go along with a decreased ability for post-shot image manipulation.

The second problem arises from the fact, that ray tracing is used for the image reconstruction, disregarding the wave nature of light. The ray tracing technique, which is used in all publications mentioned so far, is based on an approximate solution of Maxwell's equations in the limit of very short wavelengths. Therefore, ray tracing assumes incoherent superposition and ignores all diffraction effects. Such an assumption is valid for high aperture systems with large detector pixels.

The pixel sizes of modern image sensors, however, are in the order of a few wavelengths of visible light, which in combination with low aperture systems

W. Osten (ed.), *Fringe 2013*,
DOI: 10.1007/978-3-642-36359-7_14,

causes the wave field to be sampled to a degree where diffraction effects are observable in the final images. The authors of [5] present a first wave-optical approach to reconstruct an incoherently radiating object, which reconstructs almost full sensor resolution images. As a drawback, this method is also computationally very intensive.

In this talk we analyze the performance of a wave-optical image reconstruction algorithm and compare the final images to ray tracing results with respect to image quality and resolution. Furthermore, we consider the differences of these algorithms with respect to calculation performance.

2 Plenoptic Camera Principle

The basic setup of a plenoptic camera is illustrated in fig. 1. A classical imaging system (object distance g, lens focal length f1, lens diameter D1, image distance b) is followed by a micro lens array (focal length f2, pitch D2). The image sensor is positioned at a distance z behind the array.

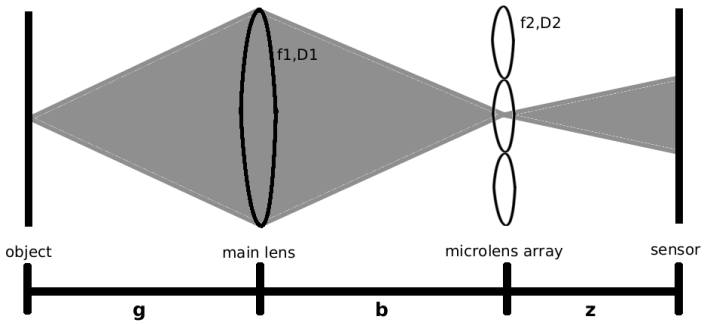

Fig. 1 Schematic sketch of the plenoptic camera setup

In the past there were mainly two suggested setups, placing the lens array either in the image plane or is used to image the latter. In this presentation, we concentrate our analysis on the following geometry: The micro lens array is placed in the image plane of the main lens (1/b+1/g=1/f1). The distance between the micro lens array and image sensor corresponds to the focal length of the micro lenses (z=f2). This is also the setup used by the authors of [1].

Due to the lack of 'real' plenoptic camera sensor data and in order to rule out reconstruction artifacts introduced by the measurement process, we created a synthetic detector image by an incoherent non-paraxial wave-optical calculation. The original object and the sensor data are shown in fig. 2.

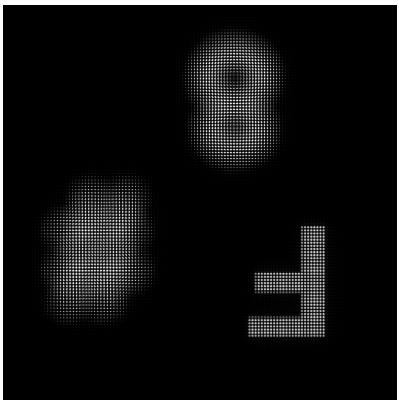

Fig. 2 Synthetic detector image created by an incoherent non-paraxial wave-optical calculation based on the setup shown in fig. 1 (f1=80mm, D1=10mm, f2=512µm, D2=64µm, b=120mm, z=f2, sensor diameter=$(8.192\text{mm})^2$, sensor resolution=4096^2 pixels). Three incoherent radiators (letters) are positioned at g=210mm ('8'), g=240mm ('F') and g=280mm ('#'). Monochromatic light at λ=633 nm is assumed.

3 Ray-Optical Reconstruction

The ray tracing approach relies on the back-propagation of rays from the sensor to an arbitrary image plane using one ray per detector pixel. For the propagation a simplified scheme using paraxial Gaussian optics is applied. The reconstructed intensity is a binned superposition of rays emitted from the sensor pixels. The binning region corresponds to the extent of the image of one micro lens.

The calculated detector image in fig. 2 serves as input for the reconstruction comparison. For the ray optical reconstruction we implemented the algorithm proposed by the authors of [1]. A reconstructed image (g=280mm) is shown in fig. 4a. For comparison of calculation speed, we performed all computations with a single CPU. In this particular case the implementation needed 330s.

4 Wave-Optical Reconstruction

The wave-optical reconstruction is based on the back-propagation of the complex wave field from the sensor to the image plane. The reconstructed intensity corresponds to the binned intensity of the reconstructed wave-field in the object plane. The binning region is the same as in the ray-optical case. Again we use the calculated detector image in fig. 2 as input.

The coherent propagation of the complex wave field is described by the Angular Spectrum (AS) method,

$$u\left(\vec{x}_\perp, z\right) = \int_{-\infty}^{\infty} \tilde{u}\left(\vec{k}_\perp, 0\right) e^{iz\sqrt{k^2 - k_\perp^2}} e^{i\vec{k}_\perp \vec{x}_\perp} \frac{d^2 k_\perp}{\left(2\pi\right)^2}, \tag{1}$$

where u is the complex wave field, z denotes the propagation distance along the optical axis, i is the imaginary unit, λ is the optical wavelength, and $k = 2\pi/\lambda$ corresponds to the wave number. The tilde stands for the 2D-Fourier transform with respect to the variable $\vec{x}_\perp$.

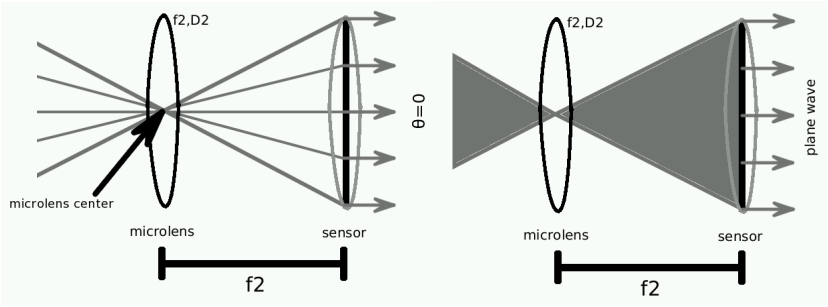

Fig. 3 Reconstruction procedure for rays (left) and the complex wave field (right) from the sensor data

The refraction by a lens (focal length f) in the thin element approximation is described by

$$u'\left(\vec{x}_\perp, z\right) = u\left(\vec{x}_\perp, z\right) e^{-\frac{i\pi}{\lambda f}\vec{x}_\perp^2}, \tag{2}$$

where u and u' are the complex wave fields before and after refraction.

The general scheme behind the wave-optical reconstruction is similar to the one used in [1]. In the latter, rays are reconstructed such that they intersect in the center of the micro lens, corresponding to the sensor pixels used as source (see fig. 3 left). Hence, in the wave-optical case, for each micro lens we start the reconstruction in the sensor plane with a converging wave, which is numerically implemented by a lens placed in the initial plane (see fig. 3 right).

Final images were calculated via intensity binning as described before. Therefore, the pixel count is the same as for ray tracing. The reconstruction (g=280mm) time was 65s and the result is shown in fig. 4b. Several weak interference artifacts are visible within the out-of-focus regions of the image, which are due to the coherent calculation. Apart from that no differences are observed.

For a better comparison with ray optics, the coherent calculation is not appropriate, since the source objects are incoherent emitters. For an incoherent calculation each object point has to be propagated separately through the optical system and the resulting intensities have to be added afterwards. This method has a very

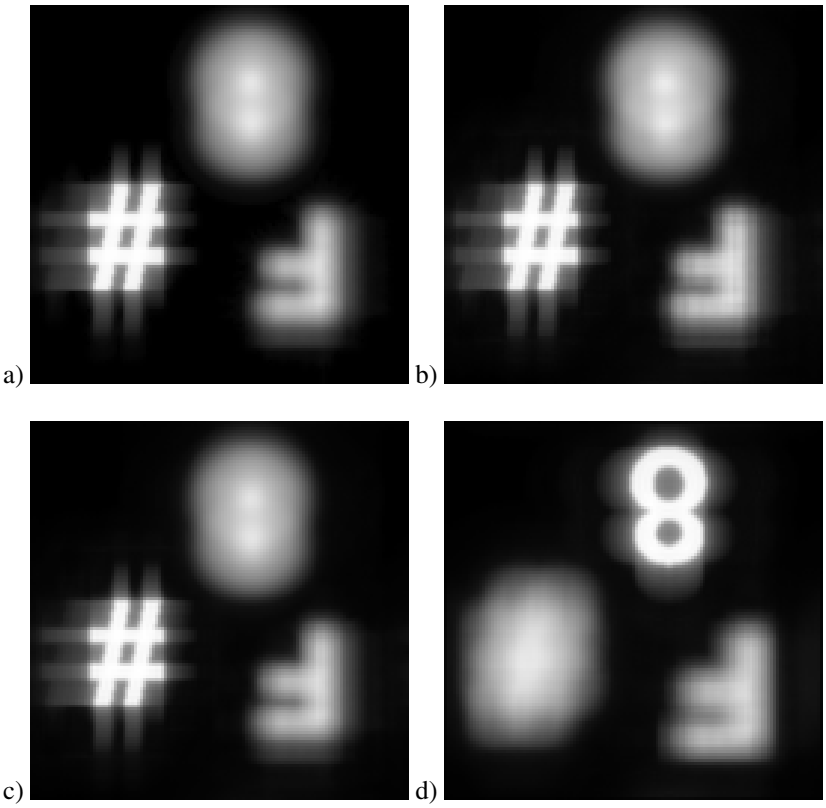

Fig. 4 Reconstruction of the data in fig. 2 using a) the ray tracing technique [1], b) coherent wave-optical propagation and c, d) partially coherent wave-optical propagation. The reconstructions a, b, c refer to the plane g=280mm, d to g=210mm.

high computational complexity. For a faster and partially coherent approach, we can propagate all pixels underneath the same micro lenses as one coherent image, but for each micro lens region we perform an incoherent superposition. This procedure can be parallelized by propagating several micro lens region in parallel, as long as their reconstructed intensities do not overlap.

The result of such a reconstruction is presented in fig. 4c. This procedure strongly reduces the interference artifacts and the image is almost identical to the result obtained by the ray tracing method. However, the computation time needed increases linearly with the number of single propagations needed. In our case four single propagations (corresponding to 195s CPU time) were already sufficient.

5 Conclusion

We compare the ray-optical reconstruction algorithm for plenoptic camera images proposed in [1] to a coherent and a partially coherent wave-optical reconstruction with respect to image quality, resolution and computational performance.

We found that the coherent wave-optical algorithm exhibits weak interference artifacts within the reconstructed out-of-focus images. The partially coherent version of the algorithm reduces these artifacts, so that eventually almost no differences to the ray-optical reconstruction algorithm are visible in the final images. The pixel count of all three methods is equal.

In our particular reconstruction using single core processing and no special optimization, the single core CPU execution times were 330s (ray-optical), 65s (coherent wave-optical) and 195s (partially coherent wave-optical).

References

1. Ng, R., Levoy, M., Brédif, M., Duval, G., Horowitz, M., Hanrahan, P.: Light field photography with a hand-held plenoptic camera. Tech. Rep. (2005)
2. Lumsdaine, A., Georgiev, T.: Full Resolution Lightfield Rendering. Tech. Rep. Adobe Systems (2008)
3. Bishop, T.E., Zanetti, S., Favaro, P.: Light field superresolution. In: Proceedings of the IEEE International Conference on Computational Photography (2009)
4. Lumsdaine, A., Georgiev, T.: Focused Plenoptic Camera and Rendering. Journal of Electronis Imaging 19(2) (2010)
5. Shroff, S., Berkner, K.: Image formation analysis and high resolution image reconstruction for plenoptic imaging systems. Applied Optics 52(10), D22–D31 (2013)